APPLIED PHYSICS

The specificity of applying the technology for ensuring magnetic purity of small spacecraft, which have cylindrical electromagnets with a magnetic moment of 10–50 A m^2 in the orbit orientation control system, has been considered. It is shown that the electromagnets of the orientation control system are the most powerful source of magnetic hindrance with a magnetic flux density of up to 1 T for the magnetically sensitive equipment of the spacecraft. The need for modeling the magnetic field of the electromagnet at the preliminary stage of spacecraft development for the rational choice of its layout has been substantiated. In order to improve the technology for ensuring magnetic purity, which is aimed at increasing the reliability of spacecraft operation, a search for the best model of the magnetic field of such electromagnets was carried out.

A comparative analysis of approximate analytical models of the near magnetic field of a cylindrical electromagnet, which are based on its magnetic moment and overall dimensions, was carried out. It is established that the model based on two shifted dipole moments and the multipole model have unacceptably large deviations in the results of calculating the near magnetic field near the body of a cylindrical electromagnet. The advantages in the form of an expanded application area and a reduced deviation of the near magnetic field representation to 5 % when using the model based on cylindrical harmonics of the electromagnet have been theoretically substantiated. Formulas for engineering calculation of the magnetic field induced by a cylindrical electromagnet inside the spacecraft using its improved analytical model have been derived. It is proposed to use the model based on cylindrical harmonics for preliminary calculation of the magnetic hindrance generated by the electromagnets of the orientation control system to the magnetically sensitive equipment of the spacecraft

Keywords: magnetic field, analytical model, cylindrical electromagnet, magnetic purity, spacecraft

UDC 621.317.4
DOI: 10.15587/1729-4061.2025.326676

IMPROVING AN ANALYTICAL MODEL OF THE NEAR MAGNETIC FIELD OF ELECTROMAGNETS IN THE SPACECRAFT ORIENTATION CONTROL SYSTEM

Andriy Getman
Corresponding author
Doctor of Technical Sciences,
Senior Researcher*
E-mail: getmanav70@gmail.com
Oleksandr Konstantinov
PhD Student*
*Department of Theoretical
Electrical Engineering
National Technical University
"Kharkiv Polytechnic Institute"
Kyrpychova str., 2, Kharkiv, Ukraine, 61002

Received 28.01.2025
Received in revised form 14.03.2025
Accepted 07.04.2025
Published 30.04.2025

How to Cite: *Getman, A., Konstantinov, O. (2025). Improving an analytical model of the near magnetic field of electromagnets in the spacecraft orientation control system. Eastern-European Journal of Enterprise Technologies, 2 (5 (134)), 6–14. https://doi.org/10.15587/1729-4061.2025.326676*

1. Introduction

The main characteristic of a stationary magnetic field source is the magnetic moment vector. It is this characteristic that determines the energy of the interaction of the source with an external magnetic field. In particular, the magnetic moment modulus is proportional to the mechanical torque that rotates the source so that the direction of the magnetic moment coincides with the lines of force of the external magnetic field. It is this interaction that is observed with the needle of a magnetic compass, which the Earth's geomagnetic field directs towards the south magnetic pole. A similar interaction between the geomagnetic field and the magnetic moment of an electromagnet is used by the orientation control systems of small spacecraft to change and stabilize their position in orbit. A spacecraft (SC) is affected by many external factors that chaotically change its standard orientation in orbit, which can cause the loss of stable communication with the satellite. Therefore, to ensure a rapid change and reliable stabilization of the angular position of SC, electromagnets are used that generate a mechanical moment significantly greater than that of the disturbance factors. It is usually necessary to generate a controlled magnetic moment of the electromagnet, the magnitude of which is approximately 100 times greater than the residual intrinsic magnetic moment of the satellite. The design of the magnetically active part of such electromagnets consists of an elongated cylindrical core and a current winding located on it. Given the significant elongation of such a magnetic moment source, the point dipole model cannot be used to calculate the near magnetic field induced by it near the electromagnet. However, there is a need to calculate the magnetic field (MF) since near the ends of the cylindrical electromagnet the magnetic flux density created by it takes values that exceed 0.5 T. Since the electromagnet of the orientation control system is the most powerful source of magnetic hindrance for the magnetically sensitive equipment of the spacecraft, the spatial distribution of its near magnetic field must be determined in advance. Determining the near magnetic field at the preliminary stage of spacecraft design is necessary for a rational, from the point of view of magnetic interaction, choice of the layout of its components and equipment.

Therefore, it seems relevant to search for and build such an analytical model of the electromagnet, which allows for engineering calculation of its near magnetic field at the stage of the preliminary design of the spacecraft. That is, at the

stage when all the design parameters have not yet been determined, and only the nominal magnetic moment and length of the electromagnet are previously known.

2. Literature review and problem statement

To ensure the reliability of the regular functioning of satellite equipment in the space industry, specially developed technologies are used. In particular, to eliminate negative magnetic interaction between individual elements, systems and payload equipment of the spacecraft, magnetic cleanliness technology is used. The methodology for applying magnetic cleanliness technology is enshrined in the standards of the European Space Agency [1, 2]. However, the standards contain only a general procedure for applying this technology, starting from the initial definition of requirements for equipment and equipment at the stage of preliminary design of the satellite. A general recommendation for modeling the magnetic field induced by the equipment and elements of the satellite is to use a convenient analytical model and previous experience in designing similar equipment. As an example of a complete algorithm for applying these standards when designing a satellite, the general sequence of ensuring magnetic cleanliness is considered in [3]. However, the strategy chosen by the developers for preliminary modeling and subsequent control is based on a multi-dipole model of the magnetic field, so the issues of taking into account the features of magnetic sources remain unresolved. Such a choice of strategy for applying technology and the model of the near-field magnetic field of components and accessories is certainly justified in the case of priority provision of regular functioning of scientific magnetometers. As an additional option for overcoming the difficulties in ensuring magnetic purity in such space missions, a remote rod is used to locate magnetometers outside the spacecraft [4–7]. This approach was used in [4] as a reliable technique that employs the property of the magnetic field decay from the source of magnetic hindrance induced by the equipment and elements of the spacecraft. However, the use of a very long mechanically collapsible rod, for example, as in the Juno mission with a length of 12 m, requires additional devices for determining the orientation of magnetometers in space. However, shorter rods are less effective, so such spacecraft require the use of additional methods of protection against magnetic hindrance [5]. For example, by using several magnetometers located and oriented according to the gradiometer scheme. In addition, an option to overcome the difficulties may be the use of special algorithms for processing magnetometer measurement data, which use information about the angular rotation of the spacecraft around its own axis [6]. However, the attempt to use a remote rod in the design of a nanosatellite weighing up to 30 kg actually makes it impossible to use other scientific instruments in the mission besides magnetometers [7].

The dominance of the multi-dipole model of magnetic hindrance sources from spacecraft components stems from the need to model the near magnetic field of all components and assemblies at the stage of preliminary design. In this case, another option for overcoming the difficulties may be the use of either estimated data on the magnetic moments of the equipment or results known from previous missions, as shown in [8]. In addition, considering the sources as magnetic dipoles, the probable approach for modeling the near magnetic field at the preliminary stage of spacecraft development may be quite effective for a series of nanosatellites of the same type [9]. An option for overcoming the difficulties in experimentally determining both the dipole magnetic moments of individual components [10] and for the entire spacecraft as a whole [11] is the use of automation, which has significantly simplified the practice of experimental control over magnetic purity.

However, the application of other models of the near magnetic field has not become widespread; the likely reason is the imperfection and limitations of the application of the multi-dipole model near the sources, which forces space technology developers to look for other approaches. For example, in [12], the overestimated degree of magnetic field decay at a distance from the real source compared to the dipole one is theoretically justified, but an attempt is made to replace it by a complex extrapolation law. A likely option for overcoming the difficulties is to use a magnetic model based on spherical harmonics of the magnetic field [13]. However, for its application. specifically determining the magnetic center and solving the inverse problem of finding an improved layout, it is necessary to have a large number of determined coefficients of the harmonics of the components and equipment of the spacecraft. In addition, the model of solar panels as a flat source of magnetic field is presented as part of the work on magnetic compatibility in [3, 14]. However, such models are based on the Biot-Savart law for the flat distribution of electric current in solar panels and are not very suitable for the calculation of electromagnets. Finally, an attempt to build an integral model for the linear distribution of magnetic moments is described in [15]. However, in this model, the magnetic moments of the spiral spring are considered to be directed perpendicular to the line of location, and the magnetization along the spring is not considered.

All this gives grounds to argue that it is advisable to conduct a study on improving the analytical model of the near-field magnetic field of elongated spacecraft components, which is based only on the dipole magnetic moment and takes into account the length of the source. This will expand the capabilities of magnetic purity technology to increase the reliability of operation of small spacecraft that have electromagnets in the orientation control system.

3. The aim and objectives of the study

The aim of our work is to improve the theoretical basis for modeling the near magnetic field of the satellite orientation system electromagnet for engineering calculation of its magnitude at the stage of preliminary design of the spacecraft. This will make it possible to increase the reliability of spacecraft operation by ensuring magnetic compatibility of individual components and satellite equipment.

To achieve the goal, the following tasks were set:

– to conduct a comparative analysis of analytical models that can be used to calculate the near magnetic field of an electromagnet with a cylindrical core;

– to derive analytical expressions for engineering calculation of the near magnetic field of the satellite orientation system using the selected model of the electromagnet as a source of magnetic moment;

– to take into account the inhomogeneous nature of the spatial distribution of magnetization in the core of the cylindrical electromagnet to improve the accuracy of the calculation of the near magnetic field induced by it.

4. The study materials and methods

The object of our study is the near-field magnetic field generated by the electromagnets of the spacecraft orientation control system. It is expected that with a limited number of known parameters of the electromagnet, the analytical model is able to describe its external magnetic field with sufficient accuracy. The work compares the accuracy of reproducing the external magnetic field of a cylindrical electromagnet by analytical models. The set of analytical models possible for application is determined by the limited number of input parameters of the electromagnet since at the initial stage of spacecraft development, only the magnetic moment M and the largest overall size of the electromagnet – its length L – can be considered known. Therefore, for comparison, the following models were considered: a model based on two shifted magnetic dipoles, a model based on magnetic multipoles, a model based on cylindrical harmonics, and a model based on spheroidal harmonics.

As a comparative basis for determining the relative deviation of the results of the analytical calculation of magnetic field by these models, the results from calculating by the numerical method were used. Numerical calculation of the magnetic field was carried out for two experimental samples of a cylindrical electromagnet (Fig. 1) manufactured at the Pivdenne Design Bureau (Ukraine).

Fig. 1. Typical image of electromagnets in the spacecraft's orientation control system

The magnetic moment of the two samples was determined by direct measurement by the magnetometric method with a deviation of 5 % on the magnetic measuring bench at the Institute of Electrical and Electronic Engineering, the National Academy of Sciences of Ukraine. During magnetic tests, the electromagnets were connected to a constant voltage source of 25 V, which generated an effective current density in the windings of 1.266 A/mm^2. The experimental samples had the same type of design of the magnetically active part of the electromagnet (Fig. 2), and their main parameters are given in Table 1.

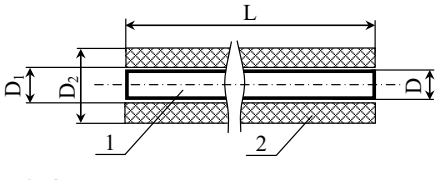

Fig. 2. Structure of the magnetically active part of the electromagnet: 1 – core; 2 – current winding

According to the data given in Table 1 and Fig. 2, two models were built in the COMSOL Multiphysics computer package for the numerical calculation of the near-field magnetic field intensity of both electromagnet samples. The results of the computer numerical calculation of the magnetic field were used for further comparison with the corresponding results obtained by analytical models. Based on the preliminary analysis of the results of the numerical calculation of the magnetic field, the following was determined.

Table 1

Parameters of experimental samples of the cylindrical electromagnet

Sample No.	Core diameter, D, mm	Minimum winding diameter, D_1, mm	Maximum winding diameter, D_2, mm	Length L, mm	Magnetic moment, M, A·m^2
1	8.5	8.7	18.2	250.0	14.13
2	10.0	10.2	19.2	300.0	23.35

Taking into account the axial symmetry of the magnetically active part of the electromagnets, the generated magnetic field has the same axis of symmetry. Therefore, to determine the deviation in the analytical simulation of the magnetic field, the two extreme directions in terms of the nature of the spatial distribution of the field were chosen. The simulation deviations were determined in the direction of the axis of symmetry, as well as in the central cross-section, as a function of the distance of the field observation point relative to the center of the electromagnet. This choice of location of observation points simplifies comparison of the results of magnetic field calculation since instead of the intensity vector, its single non-zero projection onto the applicate axis is subject to comparison.

In addition, according to a preliminary analysis of the magnetically active part of the electromagnet samples, the contribution to the external magnetic field generated by the current winding does not exceed one percent of that induced by the magnetized core. Therefore, in the analytical modeling of the magnetic field, the electromagnet was considered a permanently magnetized core with the appropriate dimensions and total magnetic moment.

5. Results of research on analytical modeling of the magnetic field

5. 1. Analytical models for calculating the near magnetic field of an electromagnet with a cylindrical core

Model based on two shifted magnetic dipoles.

For an approximate calculation of the external magnetic field of elongated magnetic moment sources, a model based on two shifted magnetic dipoles is used [16]. The model is based on two point dipoles of equal magnitude and equally directed, which are located at distances $\pm L/4$ relative to the center of the magnetized source with length L. The magnitudes of the magnetic moments of both dipoles are equal to half the magnetic moment $M/2$ of the elongated source, the field of which is being modeled.

Considering the electromagnet as a uniformly magnetized core with a magnetic moment M directed along the axial axis, the origin of the Cartesian coordinate system is placed in its center, placing the applicate axis as the axis of symmetry. According to this model, the magnetic field of an electromag-

net can be mapped in the form of representations for two projections in a cylindrical coordinate system:

$$H_\rho = \frac{3M}{8}\left\{\frac{\left(z-\frac{L}{4}\right)\rho}{\left[\rho^2+\left(z-\frac{L}{4}\right)^2\right]^{\frac{5}{2}}}+\frac{\left(z+\frac{L}{4}\right)\rho}{\left[\rho^2+\left(z+\frac{L}{4}\right)^2\right]^{\frac{5}{2}}}\right\}, \quad (1)$$

$$H_z = \frac{M}{8\pi}\left\{\frac{2\left(z-\frac{L}{4}\right)^2-\rho^2}{\left[\rho^2+\left(z-\frac{L}{4}\right)^2\right]^{\frac{5}{2}}}+\frac{2\left(z+\frac{L}{4}\right)^2-\rho^2}{\left[\rho^2+\left(z+\frac{L}{4}\right)^2\right]^{\frac{5}{2}}}\right\}, \quad (2)$$

where ρ, z are the cylindrical coordinates of the field observation point.

For the MF generated by the electromagnet in the axial direction ($\rho=0$), the model has an analytical representation for a single non-zero projection:

$$H_z = \frac{M}{4\pi}\frac{(z+L/4)^3+(z-L/4)^3}{\left(z^2-L^2/16\right)^3}. \quad (3)$$

From (2) for the projection of MF onto the axis of the applicate in the central cross-section ($z=0$) one can obtain the following representation:

$$H_z = \frac{M}{4\pi}\frac{2(L/4)^2-\rho^2}{\left[\rho^2+(L/4)^2\right]^{\frac{5}{2}}}. \quad (4)$$

To assess the accuracy of the simulation of the magnetic field in the space near the electromagnet, segments of the described two directions were selected for comparison of the results from analytical and numerical calculations. For the direction of distance relative to the center of the electromagnet along the axial axis, the magnetic field strength was compared at distances from 0.2 m to 0.5 m. In the central cross-section, the H_z projection was compared on the segment of the radial coordinate from 0.1 m to 0.5 m.

For both samples of the electromagnet in the specified directions, the relative deviation of the magnetic field simulation was calculated from the following formula:

$$\Delta = \frac{|H_0 - H_z|}{H_0}\cdot 100\,\%, \quad (5)$$

where H_0 is the MF value corresponding to the observation point, which is obtained by numerical calculation using a computer model of the electromagnet sample.

The plots of dependences of the relative deviation of MF simulation by the analytical model as a function of the distance relative to the center of the electromagnet are shown in Fig. 3.

The black lines in Fig. 3 demonstrate the accuracy of the simulation of the magnetic field of the first sample, and the red lines correspond to the dependences obtained for the second sample.

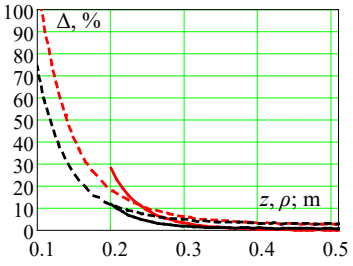

Fig. 3. Relative deviation of the application of the model based on two dipoles: dotted line – when moving away in the plane of the central cross-section, solid line – when moving away along the axial axis

Multipole model of the magnetic field of a uniformly magnetized core.

The multipole model is based on a mathematical representation of virtual point sources of the magnetic field – multipoles of power n. It is assumed that the superposition of the magnetic fields of an infinite set of multipoles with modulus M_n strictly describes the field of an arbitrary source outside the sphere that encompasses it. In the case of an axially symmetric magnetic field, the set of multipoles contains only axial multipoles of odd powers, which are directed along the axis of the applicate. In the spherical coordinate system (r, θ, φ), in the center of which are the axial multipoles, the vector of the axially symmetric magnetic field intensity has the following representation [17]:

$$\vec{H} = -\mathrm{grad}\left(\frac{1}{4\pi}\sum_{n=1}^{\infty}{}'M_n\cdot\frac{P_n(\cos\theta)}{r^{n+1}}\right), \quad (6)$$

where P_n are the Legendre polynomials of power n, Σ – sum over odd values of n.

For a uniformly magnetized cylindrical core, the moduli of axial multipoles located in its center and directed along the axial axis can be calculated from the following formula:

$$M_n = M\cdot\left(\frac{L}{2}\right)^{n-1}, \quad (7)$$

where L is the length of the core, M is the axial magnetic moment of the core.

Using (6), we can obtain a representation for the magnetic field strength along the axial axis of the electromagnet in a cylindrical coordinate system, which takes the form:

$$H = H_z = \frac{M}{4\pi}\sum_{n=1}^{\infty}{}'\left(\frac{L}{2}\right)^{n-1}\frac{n+1}{|z|^{n+2}}. \quad (8)$$

In the central cross-section, the magnetic field also has only one projection, the representation of which can be written as:

$$H_z = \frac{M}{4\pi}\sum_{n=1}^{\infty}{}'\frac{(-1)^{\frac{n+1}{2}}\,n!!(n+1)}{(n+1)!!\rho^{n+2}}\left(\frac{L}{2}\right)^{n-1}. \quad (9)$$

Having limited the infinite sums in (8) and (9) by a multipole of the tenth power, the magnetic field strength in two directions was calculated using the multipole model. For distances from 0.2 m to 0.5 m along the axial axis and from 0.1 m to 0.5 m in the central section, the relative deviation of the modeling of the magnetic field of the electromagnet by multipoles was calculated using (5) (Fig. 4).

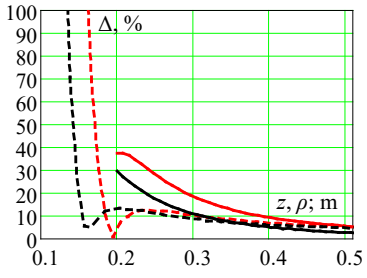

Fig. 4. Relative deviation of field modeling by multifields: dotted line — when moving away in the plane of the central cross-section, solid line — when moving away along the axial axis

The relative deviation calculations in Fig. 4 for the first sample of the electromagnet are shown by black lines, and the plots for the second sample are in red.

Model of the core of the electromagnet based on spheroidal harmonic.

Considering the nominal magnetic moment of the electromagnet as generated by its magnetized core, the modeling of its external MF by the spheroidal harmonic is considered. To apply the model, the cylindrical magnetized core is replaced by a uniformly magnetized elongated spheroid, centrally located in the elongated-spheroidal coordinate system (ξ, η, φ). In this case, the major half-axis $a=L/2$ of the spheroid is directed along the axis of the applicate, and the minor half-axis $b=D/2$ lies in the plane of the central cross-section of the electromagnet. The relationship of the triple of elongated-spheroidal coordinates with the Cartesian coordinates is given by the following formulas:

$$x=c\cdot\sqrt{\xi^2-1}\cdot\sqrt{1-\eta^2}\cdot\cos(\phi), \tag{10}$$

$$y=c\cdot\sqrt{\xi^2-1}\cdot\sqrt{1-\eta^2}\cdot\sin(\phi), \tag{11}$$

$$z=c\cdot\xi\cdot\eta, \tag{12}$$

where c is half the focal length of the spheroid, which is equal to $c=\sqrt{a^2-b^2}$.

Under these conditions, the vector of the external magnetic field of a uniformly magnetized elongated spheroid [17] is determined from the following formula:

$$\vec{H}=-\text{grad}\left(\frac{3M}{4\pi c^2}\cdot Q_1(\xi)P_1(\eta)\right), \tag{13}$$

where Q_1 is the Legendre function of the second kind; ξ, η are the spheroidal coordinates of the observation point of the magnetic field.

The spheroidal projections of the magnetic field strength obtained from (13) are converted into cylindrical projections using the following formulas [17]:

$$H_\rho=\xi\sqrt{\frac{1-\eta^2}{\xi^2-\eta^2}}\cdot H_\xi-\eta\sqrt{\frac{\xi^2-1}{\xi^2-\eta^2}}\cdot H_\eta, \tag{14}$$

$$H_z=\eta\sqrt{\frac{\xi^2-1}{\xi^2-\eta^2}}\cdot H_\xi+\xi\sqrt{\frac{1-\eta^2}{\xi^2-\eta^2}}\cdot H_\eta. \tag{15}$$

To assess the accuracy of modeling the near magnetic field with this model, formulas for direct calculation of H_z projection were derived. For the direction along the axis of the applicate, the dependence of the magnetic field strength on the z coordinate takes the following form:

$$H_z=\frac{3M}{4\pi c^3}\left[\frac{z/c}{(z/c)^2-1}-\frac{1}{2}\ln\frac{z+c}{z-c}\right]. \tag{16}$$

In the plane of the central cross-section, the magnetic field strength is a function of the radial coordinate ρ and takes the form:

$$H_z=-\frac{3M}{4\pi c^3}\left[\frac{c}{\sqrt{\rho^2+c^2}}-\frac{1}{2}\ln\frac{1+\sqrt{(\rho/c)^2+1}}{\sqrt{(\rho/c)^2+1}-1}\right]. \tag{17}$$

Using (16) and (17), for the two directions described above, the corresponding functional dependences of the magnetic field on the distance relative to the center of the electromagnet were calculated. As a result of applying (5), functions were obtained, and plots were constructed (Fig. 5) for the relative deviation of the simulation of the near magnetic field of the electromagnet based on the spheroidal harmonic.

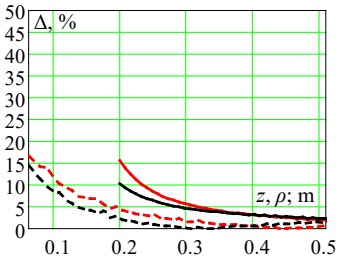

Fig. 5. Relative deviation of the model based on the spheroidal harmonic: dotted line — when moving away in the plane of the central cross-section, solid line — when moving away along the axial axis

The results of calculating the relative deviation of MF relating to the first electromagnet sample are shown in Fig. 5 by black lines, and the functions relating to the second sample are shown in red.

5. 2. Analytical representations for engineering calculation of the near magnetic field of a magnetized core of an electromagnet

The advantage of using a model based on cylindrical harmonics of the magnetic field for the case of a cylindrical source is the absence of restrictions on the external area of application of the scalar potential. For the case of a uniformly magnetized core, the simplest representations [18] of cylindrical harmonics of the external magnetic field in the direction of the axial axis are:

$$H_z=\frac{4M}{\pi^2 DL}\int_0^\infty K_1\left(\frac{\lambda D}{2}\right)\sin\left(\frac{\lambda L}{2}\right)\cos(\lambda z)\,d\lambda, \tag{18}$$

and in the central cross-section:

$$H_z=-\frac{4M}{\pi^2 DL}\int_0^\infty I_1\left(\frac{\lambda D}{2}\right)K_0(\lambda\rho)\sin\left(\frac{\lambda L}{2}\right)d\lambda, \tag{19}$$

where K_0, K_1, I_1 are modified Bessel functions, D is the diameter of the magnetized core.

To apply (18) and (19), it is necessary to have, in addition to the value of the magnetic moment and the length of the electromagnet, the value of the core diameter. It can be calculated

based on the knowledge of the magnetic properties of the material, which is usually used in the technology of manufacturing the core. For the average value of the core magnetization, in the first approximation, one can take 90 % of the maximum value of the magnetization J_s of the core material. For example, for permalloy with 50 % nickel $J_s=1.25\cdot10^6$ A/m. Considering that the magnetic moment of the core is equal to the product of the average magnetization by the volume, the following formula can be used to calculate the diameter of a cylin:

$$D=\sqrt{\frac{M}{0.9\cdot J_s}\frac{4}{\pi L}}. \tag{20}$$

To calculate both non-zero projections of the magnetic field strength using the model of cylindrical harmonics of a uniformly magnetized core at an arbitrary point (ρ, z) outside the electromagnet body, the following representations were obtained:

$$H_\rho=\frac{M}{\pi^2 DL}\frac{2}{\sqrt{2D\rho}}\left(\begin{array}{l}\left(\frac{2}{k_1}-k_1\right)K(k_1)-\frac{2}{k_1}E(k_1)-\\-\left(\frac{2}{k_2}-k_2\right)K(k_2)+\frac{2}{k_2}E(k_2)\end{array}\right), \tag{21}$$

$$H_z=\frac{M}{\pi^2 D^2 L}\frac{2\left(z-\frac{L}{2}\right)k_1}{\sqrt{2D\rho}}\left(\frac{\frac{D}{2}+\rho}{\frac{D}{2}-\rho}F(p,k_1)+K(k_1)\right)-$$
$$-\frac{M}{\pi^2 D^2 L}\frac{2\left(z+\frac{L}{2}\right)k_2}{\sqrt{2D\rho}}\left(\frac{\frac{D}{2}+\rho}{\frac{D}{2}-\rho}F(p,k_2)+K(k_2)\right), \tag{22}$$

where $K(k)$, $E(k)$, $F(p, k)$ are elliptic integrals of the first, second, and third kind, respectively. The moduli in elliptic integrals are determined from the following formulas:

$$k_1=\sqrt{\frac{2D\rho}{\left(z-\frac{L}{2}\right)^2+\left(\frac{D}{2}+\rho\right)^2}}, \tag{23}$$

$$k_2=\sqrt{\frac{2D\rho}{\left(z+\frac{L}{2}\right)^2+\left(\frac{D}{2}+\rho\right)^2}}. \tag{24}$$

To calculate parameter p of the elliptic integral of the third kind, the following formula was derived:

$$p=\frac{2D\rho}{\left(\frac{D}{2}-\rho\right)^2}. \tag{25}$$

In the resulting representations of the MF electromagnet model based on cylindrical harmonics, the real value of the core diameter is replaced by the estimated one according to (20).

5. 3. Approximate consideration of the inhomogeneous nature of the spatial distribution of magnetization in the core of a cylindrical electromagnet

To improve the accuracy of the magnetic field model based on cylindrical harmonics, it is necessary to take into account the inhomogeneous nature of the spatial distribution of magnetization in the core of the electromagnet. Considering this inhomogeneity to be generated by the inhomogeneity of the magnetic field of the current coil, it is possible to approximately calculate the effective length L_{eff} of uniform magnetization of the core, assuming this length L_{eff} equal to a segment on the axial axis of the solenoid with length L and diameter D, where the magnetic field deviates by less than 1 % from the uniform field value in the center. To use the graphical method for determining length L_{eff} we plotted (Fig. 6) the relative deviation of the magnetic field inside the solenoid Δ_{sol} from the value in the center as a function of the applicate:

$$\Delta_{sol}=\left(1-\frac{1}{2}\sqrt{\left(\frac{D}{L}\right)^2+1}\left(\begin{array}{l}\frac{1+\frac{2z}{L}}{\sqrt{\left(\frac{D}{L}\right)^2+\left(1+\frac{2z}{L}\right)^2}}+\\+\frac{1-\frac{2z}{L}}{\sqrt{\left(\frac{D}{L}\right)^2+\left(1-\frac{2z}{L}\right)^2}}\end{array}\right)\right)\cdot 100\,\%. \tag{26}$$

From the plots shown in Fig. 6, it follows that the deviation from a uniform magnetic field of up to one percent corresponds to the effective core length L_{eff} of the first sample of 0.204 m, and for the second sample L_{eff}=0.246 m. Substituting the effective core length in (18) and (19), we obtain refined representations for calculating the magnetic field along the axial axis of the electromagnet:

$$H_z=\frac{2M}{\pi D^2 L_{eff}}\times$$
$$\times\left(\frac{\frac{L_{eff}}{2}+z}{\sqrt{\left(\frac{D}{2}\right)^2+\left(\frac{L_{eff}}{2}+z\right)^2}}+\frac{\frac{L_{eff}}{2}-z}{\sqrt{\left(\frac{D}{2}\right)^2+\left(\frac{L_{eff}}{2}-z\right)^2}}\right), \tag{27}$$

and in the central cross-section:

$$H_z=-\frac{M}{\pi^2 D^2}\times$$
$$\times\frac{2}{\sqrt{\left(\frac{D}{2}+\rho\right)^2+\left(\frac{L_{eff}}{2}\right)^2}}\left(\frac{\frac{D}{2}+\rho}{\frac{D}{2}-\rho}F(p,k)+K(k)\right), \tag{28}$$

where $K(k)$, $F(p, k)$ are elliptic integrals of the first and third kind, respectively. For the central cross-section plane, the modulus k of the elliptic integrals is defined as:

$$k=\sqrt{\frac{2D\rho}{\left(\frac{D}{2}+\rho\right)^2+\left(\frac{L_{eff}}{2}\right)^2}}. \tag{29}$$

The parameter p of the elliptic integral of the third kind is given by (25).

Having calculated the magnetic field strength generated in the direction of the axial axis and in the central section by (27) and (28), the relative deviation of the field simulation by cylindrical harmonics was calculated by (5). To compare

the relative deviation of the simulation, plots were constructed (Fig. 7) for the two applied electromagnet samples.

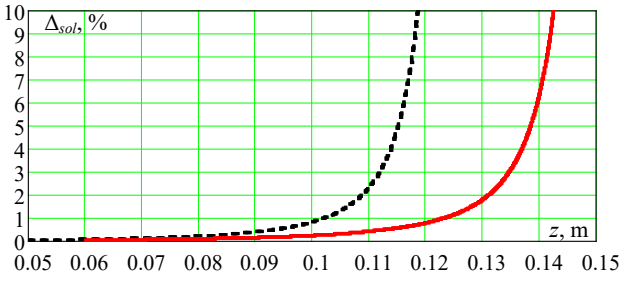

Fig. 6. Dependences of the relative deviation from a uniform field in a solenoid: the first sample of the electromagnet is the black line, the second sample is the red line

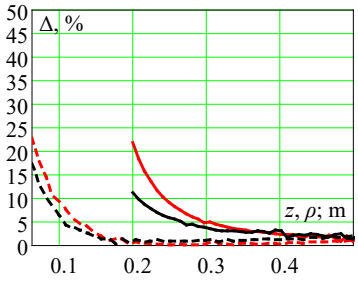

Fig. 7. Deviations when modeling the field with cylindrical harmonics: dotted line — when moving away in the plane of the central cross-section, solid line — when moving away along the axial axis

The black lines in Fig. 7 show the dependences obtained for the first sample, and the red ones for the second sample.

6. Discussion of results based on the analytical modeling of the magnetic field

The basic method of the first stage of application of the technology for ensuring the magnetic purity of the spacecraft is the modeling of the near-field magnetic field generated by its equipment and components using various analytical models of such sources [1, 2]. A common feature of the considered analytical models is the possibility of their application for calculating the magnetic field in the presence of limited information about the electromagnet that has not yet been designed and tested. Under such conditions, the discrepancy between the modeling result and the experiment is determined by many parameters (Table 1), which are not taken into account by the analytical model. However, when using the analytical model at the stage of sketch design and determination of the spacecraft layout, this feature is an important advantage over numerical calculation since the application of the numerical calculation method is not possible without complete information about the already designed or developed electromagnet.

The two electromagnet samples used for the comparison of analytical models have typical characteristics for small spacecraft with overall dimensions approaching 1 m. Therefore, the accuracy of modeling the near-field magnetic moment of the electromagnet in the range of values of distance from its body up to 0.5 m is subject to comparison. At greater distances from these electromagnet samples, it is quite sufficient to use a simpler mathematical model of one dipole magnetic moment for engineering calculation of the magnetic moment. To compare the accuracy of modeling the near-field magnetic moment by the considered analytical models, it is rational to determine the distances from the center of the electromagnet where they can be used for engineering calculation with a relative deviation of up to 5 %. In addition, it is interesting to compare the areas of incorrect estimation of the magnitude of the magnetic moment by the model with a deviation of more than 20 %.

Analyzing the plots of the relative deviation of modeling the magnetic moment by the model based on two shifted magnetic dipoles (Fig. 3), the following can be determined. For both samples of the electromagnet, engineering calculation of the MF is possible at distances from the body greater than the length of the electromagnet L. The area of correct estimation of the MF value by such a model begins at distances from the body greater than $L/2$. In this case, the modeling of MF on the side of the electromagnet has a significantly larger relative deviation than along the axial axis at the same distances to the body. This is explained by the influence of the discrete arrangement of the dipoles of the combined MF source along the axial axis of the model.

Analysis of the plots in Fig. 4 for the relative deviation of the modeling of the MF of an electromagnet by magnetic multipoles determines the mathematically prohibited area of application of the model at distances closer than $L/2$ from the center of the electromagnet. That is explained by the corresponding size of the convergence region of the multipole series when modeling the MF field outside the minimum sphere that covers the source with the maximum size L. The area for the application of the engineering calculation of MF by this model is located further from the body compared to the model based on two dipoles. The distance from the center of the electromagnet to the boundary sphere of such an area depends on the number of magnetic multipole moments used in the field calculation.

Thus, both models, which are built using point sources of the magnetic field, are not suitable for the engineering calculation of the near magnetic field of a cylindrical electromagnet. This is explained by the significant discrepancy between the shape of the real source – the cylindrical core of the electromagnet, and the turned sources that both models use.

From the comparative analysis of the plots shown in Fig. 5, 7, it follows that the best accuracy of the representation of the near-field magnetic field of the electromagnet is inherent in the model based on cylindrical harmonics. For it, the area of correct estimation of the magnitude of the magnetic field has no restrictions and begins directly behind the body of the electromagnet. In addition, with lengths of electromagnets up to 300 mm, this model can be used to calculate the magnetic field with a relative deviation of up to 5 % at distances from the body less than 0.1 m. This is explained by the improved correspondence of the cylindrical source model to the real magnetized core of the electromagnet. A possible disadvantage of this magnetic field model from the point of view of practical use is the technical difficulties in calculating according to (21) to (25). In the case of difficulties in mathematical calculation and according to simplified representations (27), (28), a model based on one spheroidal harmonic (13) to (15) can be applied, which is based exclusively on algebraic functions. In this case, the accuracy of modeling the near magnetic field will be degraded by 2–5 %, and the distances of the boundary of the region of limitation for the use of engineering field calculation are increased to $L/2$. The overall positive result when using both models is explained by

the use of an additional characteristic of the electromagnet – the expected core diameter, which is calculated based on the magnetic properties of its material according to (20).

A further area of research could be the adaptation of an improved model of the near-field magnetic field of electromagnets for its integration into computer packages for automated spacecraft design. This should simplify the search for the optimal satellite layout when solving the task to ensure its magnetic purity.

7. Conclusions

1. A comparative analysis of the relative deviation of the calculation by approximate analytical models of the near-field magnetic field of a cylindrical electromagnet has been carried out. The model based on two shifted magnetic dipoles and the model of magnetic multipole moments give an incorrect estimate of the magnitude of the magnetic field strength near the body of the electromagnet. The application of the model based on the spheroidal harmonic of a uniformly magnetized core of an electromagnet for engineering calculation of the magnetic field is possible at distances greater than half its length.

2. In order to obtain the possibility of using the cylindrical harmonic model at the initial stage of spacecraft design, a formula for the approximate calculation of the diameter of the core of an electromagnet has been theoretically substantiated. That has made it possible to derive analytical expressions based on cylindrical harmonics for engineering calculation of the magnetic field of an electromagnet, taking into account only its magnetic moment, length, and magnetic property of the core material.

3. The model of cylindrical harmonics of the magnetic field of an electromagnet has been improved by taking into account the inhomogeneous nature of the spatial distribution of magnetization in the core. For the improved model, the relative deviation of the reproduction of the near magnetic field does not exceed 5 % at distances greater than 0.1 m from the body of electromagnets with a length of up to 300 mm. This is an improvement of 2–5 % in the accuracy of analytical modeling of the magnetic field of electromagnets in the orientation control system, which is important when carrying out work to ensure the magnetic purity of spacecraft.

Conflicts of interest

The authors declare that they have no conflicts of interest in relation to the current study, including financial, personal, authorship, or any other, that could affect the study, as well as the results reported in this paper.

Funding

The study was conducted without financial support.

Data availability

All data are available, either in numerical or graphical form, in the main text of the manuscript.

Use of artificial intelligence

The authors confirm that they did not use artificial intelligence technologies when creating the current work.

Referenses

1. ECSS-E-HB-20-07A. Space engineering: Electromagnetic compatibility hand-book. ESA-ESTEC (2012). Noordwijk: Requirements & Standards Division, 228.
2. ECSS-E-HB-20-07C Rev.2. Space engineering: Electromagnetic compatibility hand-book. ESA-ESTEC (2022). Noordwijk, 116.
3. Weikert, S., Mehlem, K., Wiegand, A. (2012). Spacecraft magnetic cleanliness prediction and control. ESA Workshop on Aerospace EMC. Available at: https://www.researchgate.net/publication/241633435_Spacecraft_magnetic_cleanliness_prediction_and_control
4. Connerney, J. E. P., Benn, M., Bjarno, J. B., Denver, T., Espley, J., Jorgensen, J. L. et al. (2017). The Juno Magnetic Field Investigation. Space Science Reviews, 213 (1-4), 39–138. https://doi.org/10.1007/s11214-017-0334-z
5. Lee, J., Jin, H., Kim, K.-H., Park, H., Jo, W., Jang, Y. et al. (2023). Correction of Spacecraft Magnetic Field Noise: Initial Korean Pathfinder Lunar Orbiter MAGnetometer Observation in Solar Wind. Sensors, 23 (23), 9428. https://doi.org/10.3390/s23239428
6. de Soria-Santacruz, M., Soriano, M., Quintero, O., Wong, F., Hart, S., Kokorowski, M. et al. (2020). An Approach to Magnetic Cleanliness for the Psyche Mission. 2020 IEEE Aerospace Conference, 1–15. https://doi.org/10.1109/aero47225.2020.9172801
7. Arranz, C. J., Marchese, V., Léger, J.-M., Vallmitjana, M., Jager, T., Pous, M. (2023). Magnetic cleanliness on NanoMagSat, a CubeSats' constellation science mission. 2023 International Symposium on Electromagnetic Compatibility – EMC Europe, 1–6. https://doi.org/10.1109/emceurope57790.2023.10274205
8. Park, H. H., Jin, H., Kim, T. Y., Kim, K. H., Lee, H. J., Shin, J. H. et al. (2022). Analysis of the KPLO magnetic cleanliness for the KMAG instrument. Advances in Space Research, 69 (2), 1198–1204. https://doi.org/10.1016/j.asr.2021.11.015
9. Mentges, A., Rawal, B. S. (2022). Magnetic Dipole Moment Estimation from Nearfield Measurements Using Stochastic Gradient Descent AI Model. 2022 International Conference on Machine Learning, Big Data, Cloud and Parallel Computing (COM-IT-CON), 327–332. https://doi.org/10.1109/com-it-con54601.2022.9850855
10. Busch, S., Koss, P. A., Horch, C., Schäfer, K., Schimmerohn, M., Schäfer, F., Kühnemann, F. (2023). Magnetic cleanliness verification of miniature satellites for high precision pointing. Acta Astronautica, 210, 243–252. https://doi.org/10.1016/j.actaastro.2023.05.017
11. Dorman, C. J., Piker, C., Miles, D. M. (2024). Automated static magnetic cleanliness screening for the TRACERS small-satellite mission. Geoscientific Instrumentation, Methods and Data Systems, 13 (1), 43–50. https://doi.org/10.5194/gi-13-43-2024

12. Pudney, M. A., Carr, C. M., Schwartz, S. J., Howarth, S. I. (2013). Near-magnetic-field scaling for verification of spacecraft equipment. Geoscientific Instrumentation, Methods and Data Systems, 2 (2), 249–255. https://doi.org/10.5194/gi-2-249-2013
13. Getman, A. (2023). Improving the technology for ensuring the magnetic cleanliness of small spacecraft. Eastern-European Journal of Enterprise Technologies, 3 (5 (123)), 33–42. https://doi.org/10.15587/1729-4061.2023.282444
14. Lassakeur, A., Underwood, C. (2019). Magnetic Cleanliness Program on CubeSats for Improved Attitude Stability. 2019 9th International Conference on Recent Advances in Space Technologies (RAST), 123–129. https://doi.org/10.1109/rast.2019.8767816
15. Belsten, N. (2022). Magnetic Cleanliness, Sensing, and Calibration for CubeSats. Massachusetts Institute of Technology. Available at: https://dspace.mit.edu/handle/1721.1/143167
16. Vanderlinde, J. (2005). Classical Electromagnetic Theory. Springer Netherlands. https://doi.org/10.1007/1-4020-2700-1
17. Smythe, W. (1989). Static and Dynamic Electricity. Hemisphere Publishing Corporation, 623.
18. Getman, A. V., Konstantinov, A. V. (2013). Cylindrical harmonics of magnetic field of linear magnetized cylinder. Technical Electrodynamics, 1, 3–8. Available at: http://dspace.nbuv.gov.ua/handle/123456789/62253